Biodistribution, Cardiac and Neurobehavioral Assessments, and Neurotransmitter Quantification in Juvenile Rats following Oral Administration of Aluminum Oxide Nanoparticles

Ninell P. Mortensen[a,*], **Maria Moreno Caffaro**[a], **Purvi R. Patel**[a], **Rodney W. Snyder**[a], **Scott L. Watson**[a], **Shyam Aravamudhan**[b], **Stephanie A. Montgomery**[c], **Timothy Lefever**[a], **Susan J. Sumner**[d], **Timothy R. Fennell**[a]

[a]RTI International, 3040 E Cornwallis Road, Research Triangle Park, NC 27709, USA

[b]Joint School of Nanoscience and Nanoengineering, North Carolina A&T State University, 2907 East Gate City Blvd., Greensboro, NC 27401, USA

[c]Department of Pathology and Laboratory Medicine, The University of North Carolina at Chapel Hill, Chapel Hill, NC 27599-7525, USA

[d]UNC Nutrition Research Institute, The University of North Carolina at Chapel Hill, 500 Laureate Way, Kannapolis, NC 28081, USA

Abstract

Little is known about the uptake, biodistribution, and biological responses of nanoparticles (NPs) and their toxicity in developing animals. Here, male and female juvenile Sprague-Dawley rats received four consecutive daily doses of 10 mg/kg Al_2O_3 NP (diameter: 24 nm (TEM), hydrodynamic diameter 148 nm) or vehicle control (water) by gavage between postnatal days (PND) 17–20. Basic neurobehavioral and cardiac assessments were performed on PND20. Animals were sacrificed on PND21 and selected tissues were collected, weighed, and processed for histopathology or neurotransmitter analysis. The biodistribution of Al_2O_3 NP in tissue sections of the intestine, liver, spleen, kidney, and lymph nodes were evaluated using Enhanced Darkfield Microscopy (EDM) and Hyperspectral Imaging (HSI).

Liver-to-body weight ratio was significantly increased for male pups administered Al_2O_3 NP compared to control. HSI suggested that Al_2O_3 NP was more abundant in the duodenum and ileum tissue of the female pups compare to the male pups, while the abundance of NP was similar for male and females in the other tissues. The abundance of NP was higher in the liver compared to spleen, lymph nodes, and kidney. Homovanillic acid and norepinephrine concentrations in brain were significantly decreased following Al_2O_3 NP administration in female and male pups, while 5-hydroxyindoleacetic acid was significantly increased in male pups.

EDM/HSI indicates intestinal uptake of Al_2O_3 NP following oral administration. Al_2O_3 NP altered neurotransmitter/metabolite concentrations in juvenile rats' brain tissues. Together these data

---

*Corresponding author: Ninell P. Mortensen, Ph. D., Discovery Sciences, RTI International, 3040 Cornwallis Drive, Research Triangle Park, NC 27709, USA, nmortensen@rti.org.

suggest that orally administered Al_2O_3 NP interfere with the brain biochemistry in both female and male pups.

SHORT ABSTRACT:

Oral administration of 10 mg/kg Al_2O_3 NP between postnatal days (PND) 17–20 resulted in increased liver-to-bw ratio in male pups, indication of NP uptake, and altered neurotransmitter/ metabolite concentrations in the brain tissues in both male and female rats. Together these results suggest a low level of Al_2O_3 NP uptake following oral exposure, which adversely impact the liver in male pups, and interfere with the brain biochemistry in both female and male pups.

Keywords

INTRODUCTION

The incorporation of engineered nanomaterials (ENMs), including nanoparticles (NPs), into everyday products - such as personal care products, packaging materials, food products, water filtration units, and children's clothes and toys has resulted in unintentional oral exposure. Al_2O_3 NPs are mainly used in optics and electronics, paints, and coatings but also in areas like cosmetics, personal care products, and medicine (FutureMarkets 2013, Nanotechnologies 2019), which means that human exposure is likely to happen. Children represent a vulnerable population because perturbations in cell growth and signaling can disrupt temporally-sequenced developmental processes leading to long-term functional deficits. Little is known about the uptake, distribution, and biological responses of ENMs and their toxicity in developing animals following oral exposure.

Most early-life ENM exposure studies have examined the transfer from the exposed dam to the fetus during pregnancy, or neonatal and juvenile animal exposure via lactation. Fewer studies have investigated the direct exposure of neonate and juvenile rodents either by subcutaneous (s.c.) injection (Zhang et al. 2015), intraperitoneal (i.p.) injection (Rollerova et al. 2015), intranasal instillation (Yin et al. 2015), or inhalation (Semmler-Behnke et al. 2012). Administration of silver nanoparticle (Ag NP) s.c. to male mouse pups between postnatal days (PND) 8–21 (5 doses, 3 day intervals) produced reproductive toxicity, resulting in testicular effects (Zhang et al. 2015). Neurotoxic effects have also been reported following daily intranasal instillation of Ag NP starting in neonatal rats and continuing for 14 consecutive weeks (Yin et al. 2015), with cerebellar ataxia-like symptoms in rats, evidenced by dysfunction of motor coordination and impairment of locomotor activity (Yin et al. 2015). To the authors' knowledge, no study has investigated the uptake, biodistribution, and biological responses of ENMs following oral exposure in juvenile rats.

The homeostasis and biochemistry of the brain can be impacted through multiple routes including the bi-directional gut-brain interaction, through systemic oxidative stress, or systemic inflammation. The bidirectional gut-brain interaction is important in maintaining

gastrointestinal homeostasis and also affects motivation and higher cognitive functions {Chaudhri, 2008 #6;Cryan, 2012 #9;Mayer, 2011 #27}. Communication from the intestinal tract to the brain includes endocrine, immune, and neuronal afferent signaling. Several pathways are involved in the brain's communication to the gastrointestinal tract including the hypothalamic-pituitary-adrenal axis, the sympatho–adrenal axis, and the descending monoaminergic pathways. It is worth keeping in mind that the enteric nervous system comprises approximately 200–600 million neurons, equal to the number of neurons in the spinal cord (Mayer 2011). Interference with the bidirectional communication between the gut and the brain may lead to complications including inflammatory disorders, obesity, and eating disorders {Mayer, 2011 #26;Costa, 2000 #8}. Changes in monoamine neurotransmitter levels in brain have also been observed as a result of systemic oxidative stress {Pandey, 2015 #55} and systemic inflammation {Miller, 2013 #54;Song, 2008 #57;Abdel-Salam, 2012 #53}. Oxidative stress is when the level of free radicals and other oxidants gets so high that the oxidant homeostasis can no longer be maintained. Systemically induced oxidative stress have been shown to alter monoamine neurotransmitter levels in the brain {Pandey, 2015 #55}. Inflammatory responses induce cytokine release, and elevated systemic cytokine levels have been linked to alteration in brain monoamine neurotransmitters {Song, 2008 #57;Miller, 2013 #54}. Studies have demonstrated that cytokines can impact neurocircuits in the brain resulting in changes in motor activity, motivation, arousal, and alarm {Miller, 2013 #54}. It has not been investigated if oral exposure to ENMs during early life can interfere with the biochemistry of the brain and influence neurobehavior and neurotransmitter levels.

In this study, male and female juvenile rats were orally administered Al_2O_3 NP between PND 17–20. In this juvenile stage prior to weaning, the pups still rely on the dam's milk, but have also started to eat solid feed. The gastrointestinal tract has not yet reached the 'adult' anatomical and physiological stages {Picut, 2016 #50}, and the brain development in rats at PND 20–21 is equivalent to that of a human age 2–3 years (Semple et al. 2013). The oral route was chosen to investigate ingestion of Al_2O_3 NP, and a dose of 10 mg/kg body weight (bw) for four consecutive days were administered to the rat pups. While the mean dietary exposure to Al in children is between 0.044 – 0.123 mg/kg/day (Willhite et al. 2014) and between 0.026 – 0.03 mg/kg/day for adults (Tietz et al. 2019), no data exist for dietary Al_2O_3 NP exposure. There are, to the authors knowledge, no studies that have investigated the biological impact of orally administered Al_2O_3 NP in developing animals. Studies in adult rats and mice have tested orally administered doses that range from 0.5 – 2,000 mg Al_2O_3 NP /kg bw/dose for a duration ranging from a single dose to 6 doses/week for 13 weeks (Balasubramanyam et al. 2009, Canli and Canli 2017, Canli et al. 2019, Jalili et al. 2020, Krause et al. 2020, Park et al. 2016, Park et al. 2015, Shrivastava et al. 2014). Taking into account that developing animals may display higher sensitivity than adults, we therefore selected a subacute toxicological dose of four consecutive daily doses of 10 mg/kg bw/day Al_2O_3 NP to study the biological responses to exposure. Furthermore, selecting this dose level were guided by the formulation of a monodisperse, nanoscale Al_2O_3 NP dosing suspension.

This study was conducted as part of a National Institute of Environmental Health Sciences (NIEHS) Consortium for Nanotechnology Health Implications Research (NHIR) which

provided the Al_2O_3 NP. While Al_2O_3 NP is used in cosmetics, personal care products, and medicine (FutureMarkets 2013, Nanotechnologies 2019), there are no reports, to the authors knowledge, investigating the actual concentration or number of Al_2O_3 NP in consumer products. During exposure, bw was recorded, and after the last administered dose non-invasive measurements of basic neurobehavior and heart rate were performed. Following termination at PND 21, organ-to-bw ratio was calculated for liver and brain, the concentration of six neurotransmitters/metabolites was determined in brain tissue, and Enhanced Darkfield Microscopy (EDM) and Hyperspectral Imaging (HSI) were used to localize NPs on the cellular level in eight select tissues (duodenum, jejunum, ileum, colon, liver, spleen, lymph node, and kidney). The results presented here are basic for understanding uptake, biodistribution, and biological effects of orally administered Al_2O_3 NP in juvenile rats, and understanding gender related differences in early-life exposure.

MATERIAL AND METHODS

Nanoparticles and Chemicals

The 30 nm Al_2O_3 NP was synthesized, comprehensively characterized, and provided by Consortium Engineered Nanomaterials Resource and Coordination Core (ERCC) as part of National Institute of Environmental Health Sciences (NIEHS) Nanotechnology Health Implications Research (NHIR) consortium. The Al_2O_3 NP was synthesized by the precision flame spray pyrolysis approach and extensively characterized by Beltran-Huarac et al. (Beltran-Huarac et al. 2018). Solvents for tissue fixation included ethanol (Decon Laboratories, Inc, King of Prussia, PA), 10% buffered formalin (Thermo Scientific™ Richard-Allan Scientific, Pittsburgh, PA), and acetic acid (Fisher Scientific, Oak Ridge, TN). Neurotransmitter/metabolite standards were purchased from Sigma-Aldrich: Dopamine (DA) (Buchs, Switzerland), dihydroxyphenylacetic acid (DOPAC) (Buchs, Switzerland), 5-hydroxy-3-acetiv acid (5-HIAA) (Buchs, Switzerland), homovanillic acid (HVA) (Darmstadt, Germany), norepinephrine (NE) (St. Louis, MO), and serotonin (5-HT) (St. Louis, MO). Chemicals and solvents for neurotransmitter analysis were purchased from Alfa Aesar, Ward Hill, MA; sodium phosphate (dibasic) Na_2HPO_4 and ascorbic acid, as well as citric acid from Sigma-Aldrich, St. Louis, MO. The internal standard 3,4-dihydroxybenzylamine (DHBA) was purchased from Sigma-Aldrich, St. Louis, MO. Mobile phase solvents for neurotransmitter analysis were purchased from Sigma-Aldrich sodium phosphate (monobasic) (NaH_2PO_4) (St. Louis, MO), citric acid (St. Louis, MO), EDTA (St. Louis, MO), octanesulfonic acid (Buchs, Switzerland), and methanol from Fisher Chemicals, Ottawa, Ontario, Canada.

Formulation, Characterization and Stability Tests

The size, uniformity, and morphology of the Al_2O_3 NP were determined on a Ziess LIBRA®120 transmission electron microscope (TEM) (Carl Zeiss Microscopy, Peabody, MA). TEM samples were prepared by placing a drop of Al_2O_3 NP suspension at low density on formvar-coated TEM grids (Ted Pella, Redding, CA), followed by rinsing in DDH_2O and finally, drying at room temperature. Size distribution were measured by image analysis using ImageJ (National Institutes of Health, Bethesda, MD).

Al_2O_3 NP dosing solutions were formulated at 2 mg/mL in filtered deionized water and (Ultrasonic Liquid Processor S-4000, Misonix Inc., Farmingdale, NY) and vortexed for 30 seconds every 2 minutes as described in the 'Discrete Sonication' protocol published by Cohen et al. (Cohen et al. 2018). The hydrodynamic diameter was determined by Dynamic Light Scattering (DLS, Malvern Zetasizer Nano-ZS, Malvern Panalytical, Westborough, MA) every 2–5 minutes, until the change in NP diameter was less than 5%. The stability of the dispersed NP was measured in water after 0 and 4 hours by DLS, the NP diameter was also measured by Nanoparticle Tracker (NTA) (NanoSight LM10, Malvern Panalytical, Westborough, MA). The criteria for stability was that the hydrodynamic diameter should change <30% in a time course of 4 hours. The critical delivered sonication energy (DSE_{cr}) for the dosing solution was demined to be 1,210 J/mL. Dosing solutions were prepared freshly every day.

Housing and Dosing Administration

Sprague Dawley rat dams with their standardized litter of 5 male and 5 female pups age PND 11–12, were obtained from Charles River Laboratories (Raleigh, NC). Each dosing group had three litters, a total of 15 female and 15 male pups. The animals were handled, cared for, and used in compliance with the Guide for the Care and Use of Laboratory Animals (NRC 2011). Dams was housed with their litter in individual polycarbonate cages and fed LabDiet 5058 Breeder Diet (LabDiet, Durham, NC) and Durham City water from a reverse osmosis system was provided ad libitum. The animal room was maintained at 72 ± 3 °F, 30–70% relative humidity and a 12:12 light cycle. All rats were acclimated 5–6 days prior to initiation of dosing.

Pups were dosed daily by gavage at a concentration of 10 mg/kg Al_2O_3 NP between PND 17–20. The vehicle control group was administered an equal volume of deionized water. Each pup was weighed on the days of dosing and the appropriate volume of the dosing solution (based on body weight) drawn into the syringe. Animals were gavage-dosed using a stainless steel 22G ball-tipped gavage dosing needle and an appropriately sized syringe.

The pups were euthanized by live decapitation, since using CO_2 or anesthetic agents can cause dramatic changes in neurotransmitters (Desaulniers et al. 2011, Nakai et al. 2005). Dams were sacrificed by overexposure to CO_2.

Trunk blood samples were obtained from each pup right after decapitation in collection tubes containing EDTA to obtain plasma. The liver and brain were collected and weighed. The brain was sectioned longitudinally and placed in separate containers; the right-brain halves were used for neurotransmitter/metabolite analysis. The liver, spleen, kidney, mesenteric lymph nodes, small intestine and colon from 12 pups per dose group (2 male and 2 female pups per litter from three litters) were collected for histopathology.

Neurobehavioral Assessment Test

The motor activity test was done using the Photobeam Activity System (PAS) (San Diego Instruments, San Diego, CA). The photobeam test is designed to assess the locomotor activity using the collection and recording of beam breaks over time as the animal moves. Locomotor activity was tested on PND 20, 4 hours after the last dose was administered to

the pups and recorded for 10 minutes in two intervals; Interval 1: 0:00–5:00 minutes and Interval 2: 5:01–10:00 minutes. Locomotor activity testing was performed for a total of eight male and eight female pups across the three litters. The locomotor activity testing was conducted at the same time for male and female pups.

The Startle Response System Test (San Diego Instruments SR-Lab chambers, San Diego, CA) was performed on PND 20, 4 hours after administration of the last dose, for a total of eight male and eight female pups from three litters. The acoustic startle response testing was conducted at the same time for male and female pups. The session started after 5 minutes (300 seconds) acclimation period where pups were exposed to background noise of 69dB, followed by the accuostic startle as a single pulse of 120 dB. Accoustic startle was measured as Time to Max Peak (msec), Average Peak (mV), and Max Peak (mV).

The Rotarod test was performed using a Stoelting Rotarod, model 52790, using a 1¼ inch diameter drums (Stoelting, Wood Dale, IL). The test was completed when all pups fell off the rod, or when 150 seconds had expired, and the rod stopped moving. Rotarod was performed on PND 20, 4 hours after administration of the last dose, for a total of 8 male and 8 female pups from three litters. The Rotarod testing was conducted at the same time for male and female pups. Rotarod performance was measured as time to fall (sec) and distance to fall.

Cardiac Assessment

Cardiac repolarization (electrocardiograms [ECG]) was measured by ECGenie (Mouse Specific, Inc, Framingham, MA) on PND 20, 4 hours after the last dose was administered to the pups. ECGenie was done for a total of seven male and seven female pups from three litters. The ECGenie testing was conducted at the same time for male and female pups. The ECGenie detects cardiac electrical activity through the animals' paws, using a shielded acquisition platform, analog input and bioamplification, and direct connection to a computer with the data acquisition software (LabChart8). The pups were placed on the platform for 10 minutes to allow them to acclimate and to record good quality ECGs. A minimum of five good quality ECG sequences were analyzed for each pup and the mean echocardiographic parameters calculated.

Histopathology

Tissue collected for histopathology were fixed in 10% buffered formalin (Thermo Scientific™ Richard-Allan Scientific, Pittsburgh, PA) for 72 hours, washed briefly in deionized water and transferred to 70% ethanol until processed. Intestinal duodenum, jejunum, ileum, and colon tissue were prepared using the improved Swiss roll technique, following the published protocol (Bialkowska et al. 2016). In short, each of the four intestinal sections were flushed with 10 mL of modified Bouin's fixative (50% ethanol/5% acetic acid in dH_2O). The rinsed tissues were cut open longitudinally along the mesenteric line and rolled from the proximal to the distal end with the lumen facing up. Tissues were imbedded, sectioned and stained at Lineberger Comprehensive Cancer Center Animal Histopathology Core, University of North Carolina Chapel Hill, Chapel Hill, NC. Duodenum, jejunum, ileum, colon, liver, spleen, and lymph node were examined by

hematoxylin and eosin (H&E) histologic staining under Olympus BX43 light microscopy (Olympus, Waltham, MA).

Biodistribution of Al$_2$O$_3$ NP in tissue

H&E stained tissue sections from dosed and control animals were imaged using a near-inferred enhanced darkfield microscope (EDM) with a hyperspectral imaging (HSI) unit (CytoViva Inc., Auburn, Al). The microscope includes a standard BX41 Olympus microscope, dark field condenser, and HSI unit. Images were first collected using darkfield microscopy, software Q-Capture 7, followed by HSI, software ENVI 4.8. Images were collected using a 60x oil objective. At least five images were collected for each tissue section per animal from three male and three female pups, resulting in a total of 15 images per tissue per gender. Spectral Libraries (SL) were built for each of the eight tissues. Each library was filtered against at least five images of the corresponding control tissue to remove any spectra not specific to Al$_2$O$_3$ NP. The filtered SL was used to map the location of spectra unique to NPs in each image using the ENVI 4.8 software. The images of mapped spectra overlaid on the original hyperspectral image was saved as a separate file. The number of NP signals were counted using ImageJ (NIH), these signals could correspond to individual or small aggregates of NPs. The presence of NPs in the tissues were scored: 0 = no NP signals detected; 1 = 1 – 10 NP signals detected; 2 = 11 – 25 NP signals detected; 3 = 26 – 50 NP signals detected; 4 = 51 – 100 NP signals detected; 5 = >100 NP signals detected. For the four intestinal sections the presence of NPs was evaluated in the lumen and tissue separately.

Quantification of Neurotransmitter and Metabolite in Brain Tissue

The concentration of six monoamine neurotransmitters/metabolites related to memory, emotion, depression, anxiety, and neuroendocrine function was quantitated in the right brain half from male and female pups: dopamine (DA), dihydroxyphenylacetic acid (DOPAC), homovanillic acid (HVA), norepinephrine (NE) (also called noradrenaline [NA] or noradrenalin), serotonin (5-HT), and 5-hydroxy-3-acetic acid (5-HIAA) using ultra high pressure liquid chromatography (UPLC) coupled with electrochemical detection (ECD). Brain tissues for vehicle control and Al$_2$O$_3$ NP exposed male and female pups were collected at the same time during the day, eliminating possible confounding neurotransmitter/metabolite levels due to diurnal variance. Brain tissues for neurotransmitter/metabolite analysis were prepared in tissue buffer consisting of 0.05 M Na$_2$HPO$_4$, 0.03 M citric acid, and 2 mM ascorbic acid at pH 3. Internal standard solution was prepared with DHBA at 200 ng/mL in tissue buffer. Internal standard or tissue buffer solution was then added to each sample at a ratio of 5 mL per g of brain tissue. Extraction of neurotransmitters/metabolites from brain tissues was conducted by adding ten, 2.8 mm stainless steel grinding balls to each sample for homogenization. Samples were homogenized by two, 30 second cycles on a Geno/Grinder 2010 (SPEX SamplePrep, Metuchen, NJ). Samples were then centrifuged at 3,500 x g for 10 minutes at 4 °C. Aliquots of supernatant were taken and passed through an Ultrafree®-MC 0.45 μm Polyvinylidene Fluoride (PVDF) filter (Merck Millipore Ltd., Tullagreen Carrigtwohill, Co. Cork, IRL). The processed samples were analyzed by injecting a 10 μL aliquot onto a Luna Omega 1.6 μm Polar C18, 2.1 × 150 mm column (Phenomenex, Torrance, CA) coupled to a LPG-3400RS pump, WPS-3000TBRS autosampler, and a 5600A CoulArray electrochemical

detector (Thermo Scientific, Waltham, MA). The column was heated to 32 °C. The mobile phase consisted of 50 mM sodium phosphate, 47 mM citric acid, 0.14 mM EDTA, 0.64 mM octanesulfonic acid, and 5% methanol, at a flow rate of 0.4 mL/min. The detector was set to sequentially deliver potentials of −150 mV, 150 mV, 400 mV, and 600 mV for this analysis.

Statistical Analysis

Test for equality of variances was performed prior to statistical analysis, and t-test for equal or unequal variance was used accordingly. An unpaired, two-tailed t-test (equal variance) or a t-test with Welch correction (unequal variance) were used for statistical analysis between doing groups using the software GraphPad Prism 7.04 (GraphPad Software, San Diego, CA).

RESULTS

Nanoparticle Characterization

The Al_2O_3 NP provided by NIEHS NHIR was characterized by TEM (Figure 1A–B). TEM analysis showed a diameter of 23.8 ± 12.1 nm. The 2 mg/mL dosing solution was characterized by DLS and NTA over a period of 4 hours (Figure 1C). The results showed a monodisperse NP suspension with a stable hydrodynamic diameter over a time course of 4 hours.

Body Weight (bw) and Organ-to-bw Ratio

No significant difference in bw was observed between the Al_2O_3 NP dosing group and the vehicle control for either male of female pups over the cause of the study (Figures 2A and 2D). The liver-to-bw ratio was significantly increased following Al_2O_3 NP administration for male pups ($P = 0.0294$), but not in female pups (Figures 2B and 2E). No changes were observed for brain-to-bw ratio for either gender (Figures 2C and 2F).

Neurobehavioral and Cardiac Assessment

Three basic neurobehavioral assessments were performed on PND 20; locomotor activity, acoustic startle and rotarod (Figure 3). Locomotor activity was measured as total beam break and recorded as a 10 minute session with two intervals, 00:00 – 05:00 and 05:01 – 10:00. No significant changes were observed for either of the two intervals (data not shown) or for the 10 minutes session (Figures 3A and 3D). Acoustic startle response for the pups was measured as time to max peak (msec) (data not shown), average of peaks (mV) (data not shown), and max peak (mV) following a single acoustic startle (Figures 3B and 3E). Al_2O_3 NP exposure did not impact acoustic startle response. Rotarod performance was measured as distance to fall (data not shown) and time to fall (sec) (Figures 3C and 3F). Administration of Al_2O_3 NP led to a significant increase in both distance to fall ($P = 0.0310$) and time to fall for female pups ($P = 0.0141$), but not in male pups.

The ECGs of unrestrained and awake pups were obtained non-invasively (Figure 4). While there was a trend in male pups that the mean heart rate (beats per minute [bpm]) were increased for Al_2O_3 NP (535 ± 27.2 bpm), the difference was not significant from the vehicle control (508 ± 35.7 bpm) (Figure 4A). Also, for female pups the mean heart rate was

slightly higher for Al_2O_3 NP (533 ± 35.0 bpm) compared to the vehicle control (512 ± 46.0 bpm) (Figure 4B). RR and ST intervals were not significantly impacted by Al_2O_3 NP (Figure 4C–F).

Biodistribution of Al_2O_3 NP

EDM and HSI was used to evaluate the biodistribution of Al_2O_3 NP in H&E stained duodenum, ileum, jejunum, and colon (Figure 5) and liver, spleen, lymph node, and kidney (Figure 6) and the abundance of NP signals per images was scored (Figure 5I and Figure 6 I). Hyperspectal libraries were built for each tissue and filtered against several images of their respectable control tissue, using multiple areas from each tissue in order to filter the libraries against a representative selection of spectra. The resulting libraries comprise spectra unique to the Al_2O_3 NP exposed tissues, were used to map the location of NP. It should be noted, that HSI mapping of unique spectra could, in addition to Al_2O_3 NP, also capture changes in tissue due to exposure such as inflammation, apoptosis, necrosis etc. To ensure that the unique spectra were not caused by e.g. inflammation, apoptosis, necrosis, pathological evaluation were done under light microscopy and was found to be within normal limits for the eight tissues. A mild to occasionally moderate lymphocytic portal hepatitis focused on bile ductules is present across all groups. We therefore assume that the HSI libraries mapped the location of Al_2O_3 NP.

Al_2O_3 NP was found in lumen, ducts, crypts, and intestinal tissue of duodenum, jejunum, ileum, and colon (Figure 5). The mucus layer was not preserved using the Swiss Roll technique, so this report cannot speak to the presence or retention of Al_2O_3 NP in the mucus layer. In the duodenum and jejunum tissue, Al_2O_3 NP was most frequently located in the lamina propria and muscularis mucosa, but also found in villi enterocytes and muscularis externa. In the ileum, Al_2O_3 NP was also located in Peyer's Patches as well as lamina propria and muscularis mucosa. In the colon tissue, Al_2O_3 NP was most frequently located in the lamina propria and muscularis mucosa, and to a lesser extent in muscularis externa. The score for duodenum tissues was significantly higher for female (2.5 ± 1.3) than male (1.3 ± 0.59) pups (P-value = 0.0020), as was the score for ileum, female (2.2 ± 0.9) than male (1.2 ± 1.1) pups (P-value = 0.021). While low levels of Al_2O_3 NP were observed in the washed lumen of the small intestine, none were present in the large intestine.

In hepatic tissue (Figure 6A–B), Al_2O_3 NP was found in hepatocytes in most images, but also frequently in Kupffer cells, and occasionally in small blood vessels. Al_2O_3 NP was found in low levels throughout the spleen, lymph nodes, and kidneys (Figure 6C–H). The score for spleen was slightly, but significantly, higher for female (1.3 ± 0.49) than male (1.0 ± 0.38) pups (P-value = 0.0457) (Figure 6I).

Neurotransmitter/Metabolite Concentrations in Brain

The concentrations of six neurotransmitters/metabolites were determined in the right brain half for male and female pups (Figure 7). HVA and NE were significantly decreased in male and female pups dosed with Al_2O_3 NP, while 5-HIAA were significantly increased in male pups, but not female. No significant changes were found for 5-HT, DA and DOPAC.

DISCUSSION

The global production volume of Al_2O_3 NP was estimated to be between 20,000 – 42,000 tons in 2012 with majority of the demand in areas of paints, coatings, and electronics, but also a considerable percentage (25%) in cosmetics, personal care products, food, and medical applications (FutureMarkets 2013). The study presented here focuses on the impact of orally administration of Al_2O_3 NP during early life in rats. Juvenile rats received four daily (PND 17 – 20) consecutive doses of Al_2O_3 NP and were sacrificed 24 hours after the last dose was administered. The biodistribution of Al_2O_3 NP, changes in basic neurobehavioral and cardiac performance, and impact on neurotransmitter/metabolite concentrations in the brain were investigated in both male and female juvenile rats.

The gastrointestinal tract undergoes significant development during early life. The stomachs of neonates and juvenile rats have considerable anatomical and physiological differences from those of adults (Hervatin et al. 1989, Picut and Coleman 2016). At PND 21, anatomically the cell population and differentiation are comparable to the adult stomach, however, significant acid secretion and pepsinogen activation occurs around weaning (Picut and Coleman 2016). In this report, juvenile rats were dosed between PND 17–20, before weaning, when the pups are still dependent on the dam's milk but have started to eat solid feed as well. In the intestine there is a close relation between the degree of maturation and absorptive functions (Pacha 2000). Permeability of the immature intestine is higher than in adults (Wisser and Horster 1978), and the response of the intestine to hypertonic perfusion is age-dependent (Younoszai et al. 1978), indicating that paracellular pathways might change with development. The initial high permeability of the intestinal epithelium for macromolecules declines after birth, a process commonly referred to as "gut closure", which is completed in rats around PND 21 (Drozdowski et al. 2010, Lecce and Broughton 1973, Teichberg et al. 1992, Westrom et al. 1982, Westrom et al. 1989). In the investigation described here, male and female rats were administered Al_2O_3 NP before "gut closure" was fully complete and the anatomically and chemical composition of tissue and gastrointestinal fluids had reached the adult state.

In the study presented here we tested a spherical-shape Al_2O_3 NP, with a hydrodynamic diameter of 148 ± 1.3 nm in dH_2O and evaluate the biodistribution in eight tissues. EDM/HSI has successfully been used in the literature for NP biodistribution evaluations in rodents (Austin et al. 2015, Guttenberg et al. 2016, Husain et al. 2015, SoRelle et al. 2016), including rats exposed via inhalation to Al_2O_3 NP (Guttenberg et al. 2016). Other reports of Al_2O_3 NP tissue distribution in adult mice and rats have tested NP with similar hydrodynamic dimeter (Al_2O_3-30 nm: 212 and Al_2O_3-40 nm: 226 nm) in MiliQ H_2O (Balasubramanyam et al. 2009), larger hydrodynamic diameter of 786 ± 94 nm in dH_2O (Park et al. 2016), rod-shape morphology (Krause et al. 2020, Park et al. 2015), and difference surface charge (Balasubramanyam et al. 2009, Park et al. 2016, Park et al. 2015). However, despite these variations in Al_2O_3 NP physiochemical properties, intestinal uptake was evident by ICP-MS analysis of tissues (Balasubramanyam et al. 2009, Krause et al. 2020, Park et al. 2016, Park et al. 2015). Interestingly, Krause et al (2020) found a higher intestinal uptake following oral dosing of rod-shape Al_2O_3 NPs (10 nm wide and 20 – 50 nm long) than soluble aluminum salt ($AlCl_3 \cdot 6H_2O$). Using a combination of EDM and HSI, we

here mapped the location of Al_2O_3 NP exposure tissue in the three sections of the small intestine (duodenum, jejunum, and ileum) and the large intestine (colon). While unique spectra could also have been attributed by tissue changes, no histopathological changes were observed. Al_2O_3 NP was present in most of the collected images and, interestingly, in a significantly higher level in female duodenal and ileum tissue compared to males. This could suggest that the uptake in duodenum is higher in female pups compared to male pups, however, the level of Al_2O_3 NP in the four internal organs examined (liver, spleen, kidney, and lymph nodes) were similar between male and female pups. Of these other organs, liver had the highest occurrence of Al_2O_3 NP, which corresponds with substances absorbed into the portal circulation are carried directly to the liver, making the liver the first line of defense against circulating NPs. Spherical NPs have been shown to accumulate in the liver of adult animals (Fennell et al. 2016, Kim et al. 2008, Kumari et al. 2014, Lee et al. 2013, Loeschner et al. 2011) and are hypothesized to cause oxidative stress and damage (Nel et al. 2006, Nel et al. 2013). In this study, the liver-to-bw ratio increased significantly in male pups following oral administration of Al_2O_3 NP, while no change was observed for the liver-to-bw ratio in females. Organ weight is considered a sensitive indicator of toxicity (Michael et al. 2007, Piao et al. 2013). Changes in liver-to-bw ratio, as a predictive endpoint for accurately detecting organ toxicity, has been demonstrated in a study analyzing the data for control animals from 26 toxicity studies conducted under similar conditions (Bailey et al. 2004). The increase liver-to-bw ratio found in the study presented here, therefore encourages further investigations of the short-term and long-term impact on hepatic health and function following early life exposure to Al_2O_3 NP.

Aluminum is a known neurotoxin, however Al_2O_3 NP is considered a stable NP that does not undergo dissolution at pH above 3 (Changmai et al. 2017). The pH of the rat stomach at PND 21 is approximately 4, suggesting that the dissolution of Al_2O_3 NP in the study here was negligible. Our EDM/HSI results suggest intestinal uptake of Al_2O_3 NP in juvenile rats, which is supported by published findings in adult mice and rats (Balasubramanyam et al. 2009, Krause et al. 2020, Park et al. 2016, Park et al. 2015). The permeability of the developing blood-brain-barrier (BBB) in fetuses and neonates has been a subject of intense debate over the past decades, and reviews indicate that the developing BBB is not more permeable than that of adults, but is a significant, functional barrier early on (Saunders et al. 2014, Saunders et al. 1999, Saunders et al. 2012). In addition to the ongoing development of the intestinal tract, the brain and central nervous system also undergo considerable development during the neonatal and juvenile life stages (Ingber and Pohl 2016, Lenz et al. 2012, Semple et al. 2013). The results presented here show that neurotransmitter/metabolite concentrations in the brain were impacted by oral administration of Al_2O_3 NP. In male juvenile rats the concentration of 5-HIAA was significantly increased following exposure, while HVA and NE concentrations were significantly decreased in both male and female juvenile rats. Other studies have also looked at the effect of NPs on neurotransmitters/metabolites in adult rodents {Hu, 2010 #17;Amara, 2014 #2;Shrivastava, 2014 #42}. Adult female mice dosed orally with 5 mg/kg TiO_2 NP for 60 days had decreased levels of DA in the brain, while a dose of 50 mg/kg led to decreased concentrations of all five tested neurotransmitters/metabolites: NE, DA, DOPAC, 5-HT, and 5-HIAA {Hu, 2010 #17}. In contrast, when 500 mg/kg TiO_2 NP, ZnO NP, or Al_2O_3 NP were orally administered to adult

male mice for 21 days, NE and DA concentrations in the cortex region of the brain increased, while 5-HT concentration were unaltered {Shrivastava, 2014 #42}. Collectively, these data suggest that NPs can impact the concentrations of neurotransmitters and their metabolites in the brain following oral exposure and that more work is needed to understand the underlying mechanisms and effects. The neurotransmitter/metabolite results presented here indicate that Al_2O_3 NP may interfere with the gut-brain axis in developing animals. However, since nanoparticles can induce both oxidative stress and inflammatory responses (Nel et al. 2006, Nel et al. 2013), and alterations in the levels of monoamine neurotransmitter in the brain has been reported as a result of both oxidative stress (Pandey et al. 2015) and inflammation (Abdel-Salam et al. 2012, Miller et al. 2013, Song et al. 2008). It is also possible that orally administered Al_2O_3 NP may cause an increase in systemic levels of oxidative stress markers and/or cytokines in juvenile rats which can influence the neurotransmitter levels in the brain. The long-term consequences of such an interference with the biochemistry of the brain needs further investigation, especially in developing animals.

No changes were observed for locomotor activity or acoustic startle response, but female pups administered Al_2O_3 NP did, surprisingly, perform better in the Rotarod test than vehicle controls. The Rotarod test assess the rat pups motor coordination, grip strength and balance, and the findings presented here suggest that Al_2O_3 NP lead to an improve performance. The underlying mechanisms need to be investigated further to explain these results. It should also be noted that changes in neurobehavioral outcome is likely dependent on molecular and/or cellular events and could be delayed. Carr et al (2001) did not observe a decrease locomotor activity in the open-field behavior test before PND 25 and PND 30 in juvenile rat dosed with the organophosphorus insecticide chlorpyrifos every second day between PND 1 – 21 (Carr et al. 2001). It can therefore not be ruled out that neurobehavioral effect, as a result of early-life exposure to Al_2O_3 NP, could happen at a later age.

In this early-life investigation of the biological impact of orally administered Al_2O_3 NP in juvenile male and female rats we found evidence of NP interference with the biochemistry in the brain by altering the neurotransmitter/metabolites concentrations in the brain tissue. It was also evident that some responses to exposure are gender specific. Liver-to-bw ratio was only increased in male rats, while the occurrence of Al_2O_3 NP in liver tissues were similar between genders, suggesting an increased hepatic sensitivity in male juvenile rats. The results presented in this report demonstrate the importance of investigating oral ENMs exposure during early-life and that more research is needed in this area to understand the long-term consequences. Scientific data of early-life exposure is critical for nanosafety and risk evaluation of oral exposure in infants and young children.

Supplementary Material

Refer to Web version on PubMed Central for supplementary material.

ACKNOWLEDGEMENT

REFERENCE

Abdel-Salam OM, Salem NA, Hussein JS. 2012. Effect of aspartame on oxidative stress and monoamine neurotransmitter levels in lipopolysaccharide-treated mice. Neurotox Res 21:245–255. DOI: 10.1007/s12640-011-9264-9. [PubMed: 21822758]

Amara S, Ben-Slama I, Mrad I, Rihane N, Jeljeli M, El-Mir L, Ben-Rhouma K, Rachidi W, Seve M, Abdelmelek H, Sakly M. 2014. Acute exposure to zinc oxide nanoparticles does not affect the cognitive capacity and neurotransmitters levels in adult rats. Nanotoxicology 8 Suppl 1:208–215. DOI: 10.3109/17435390.2013.879342. [PubMed: 24524369]

Austin CA, Hinkley GK, Mishra AR, Zhang Q, Umbreit TH, Betz MW, B EW, Casey BJ, Francke-Carroll S, Hussain SM, Roberts SM, Brown KM, Goering PL. 2015. Distribution and accumulation of 10 nm silver nanoparticles in maternal tissues and visceral yolk sac of pregnant mice, and a potential effect on embryo growth. Nanotoxicology, 10.3109/17435390.2015.1107143:1–8. DOI: 10.3109/17435390.2015.1107143.

Bailey SA, Zidell RH, Perry RW. 2004. Relationships between organ weight and body/brain weight in the rat: what is the best analytical endpoint? Toxicologic pathology 32:448–466. DOI: 10.1080/01926230490465874. [PubMed: 15204968]

Balasubramanyam A, Sailaja N, Mahboob M, Rahman MF, Hussain SM, Grover P. 2009. In vivo genotoxicity assessment of aluminium oxide nanomaterials in rat peripheral blood cells using the comet assay and micronucleus test. Mutagenesis 24:245–251. DOI: 10.1093/mutage/gep003. [PubMed: 19237533]

Beltran-Huarac J, Zhang Z, Pyrgiotakis G, DeLoid G, Vaze N, Hussain SM, Demokritou P. 2018. Development of reference metal and metal oxide engineered nanomaterials for nanotoxicology research using high throughput and precision flame spray synthesis approaches. NanoImpact 10:26–37. DOI: 10.1016/j.impact.2017.11.007. [PubMed: 30035243]

Bialkowska AB, Ghaleb AM, Nandan MO, Yang VW. 2016. Improved Swiss-rolling Technique for Intestinal Tissue Preparation for Immunohistochemical and Immunofluorescent Analyses. J Vis Exp, 10.3791/54161. DOI: 10.3791/54161.

Canli EG, Canli M. 2017. Effects of aluminum, copper, and titanium nanoparticles onsome blood parameters in Wistar rats. Turkish Journal of Zoology 41:259–266. DOI: 10.3906/zoo-1512-23.

Canli EG, Ila HB, Canli M. 2019. Responses of biomarkers belonging to different metabolic systems of rats following oral administration of aluminium nanoparticle. Environmental toxicology and pharmacology 69:72–79. DOI: 10.1016/j.etap.2019.04.002. [PubMed: 30965278]

Carr RL, Chambers HW, Guarisco JA, Richardson JR, Tang J, Chambers JE. 2001. Effects of repeated oral postnatal exposure to chlorpyrifos on open-field behavior in juvenile rats. Toxicol Sci 59:260–267. DOI: 10.1093/toxsci/59.2.260. [PubMed: 11158719]

Changmai M, Priyesh JP, Purkait MK. 2017. Al 2 O 3 nanoparticles synthesized using various oxidizing agents: Defluoridation performance. Journal of Science: Advanced Materials and Devices 2:483–492. DOI: 10.1016/j.jsamd.2017.09.001.

Chaudhri OB, Salem V, Murphy KG, Bloom SR. 2008. Gastrointestinal satiety signals. Annual review of physiology 70:239–255. DOI: 10.1146/annurev.physiol.70.113006.100506.

Cohen JM, Beltran-Huarac J, Pyrgiotakis G, Demokritou P. 2018. Effective delivery of sonication energy to fast settling and agglomerating nanomaterial suspensions for cellular studies: Implications for stability, particle kinetics, dosimetry and toxicity. NanoImpact 10:81–86. DOI: 10.1016/j.impact.2017.12.002. [PubMed: 29479575]

Costa M, Brookes SJ, Hennig GW. 2000. Anatomy and physiology of the enteric nervous system. Gut 47 Suppl 4:iv15–19; discussion iv26. [PubMed: 11076898]

Cryan JF, Dinan TG. 2012. Mind-altering microorganisms: the impact of the gut microbiota on brain and behaviour. Nature reviews. Neuroscience 13:701–712. DOI: 10.1038/nrn3346. [PubMed: 22968153]

Desaulniers D, Yagminas A, Chu I, Nakai J. 2011. Effects of anesthetics and terminal procedures on biochemical and hormonal measurements in polychlorinated biphenyl treated rats. International journal of toxicology 30:334–347. DOI: 10.1177/1091581810397774. [PubMed: 21444927]

Drozdowski LA, Clandinin T, Thomson ABR. 2010. Ontogeny, growth and development of the small intestine: Understanding pediatric gastroenterology. World J Gastroenterol 16:787–799. DOI: 10.3748/wjg.v16.i7.787. [PubMed: 20143457]

Fennell TR, Mortensen NP, Black SR, Snyder RW, Levine KE, Poitras E, Harrington JM, Wingard CJ, Holland NA, Pathmasiri W, Sumner SC. 2016. Disposition of intravenously or orally administered silver nanoparticles in pregnant rats and the effect on the biochemical profile in urine. J Appl Toxicol, 10.1002/jat.3387. DOI: 10.1002/jat.3387.

FutureMarkets. 2013. THE GLOBAL MARKET FOR ALUMINIUM OXIDE NANOPARTICLES. Future Markets I (ed).

Guttenberg M, Bezerra L, Neu-Baker NM, Del Pilar Sosa Idelchik M, Elder A, Oberdorster G, Brenner SA. 2016. Biodistribution of inhaled metal oxide nanoparticles mimicking occupational exposure: a preliminary investigation using enhanced darkfield microscopy. J Biophotonics 9:987–993. DOI: 10.1002/jbio.201600125. [PubMed: 27528427]

Hervatin F, Moreau E, Ducroc R, Garzon B, Geloso JP. 1989. Development of acid secretory function in the rat stomach: sensitivity to secretagogues and corticosterone. Journal of pediatric gastroenterology and nutrition 9:82–88. [PubMed: 2550602]

Hu R, Gong X, Duan Y, Li N, Che Y, Cui Y, Zhou M, Liu C, Wang H, Hong F. 2010. Neurotoxicological effects and the impairment of spatial recognition memory in mice caused by exposure to TiO2 nanoparticles. Biomaterials 31:8043–8050. DOI: 10.1016/j.biomaterials.2010.07.011. [PubMed: 20692697]

Husain M, Wu D, Saber AT, Decan N, Jacobsen NR, Williams A, Yauk CL, Wallin H, Vogel U, Halappanavar S. 2015. Intratracheally instilled titanium dioxide nanoparticles translocate to heart and liver and activate complement cascade in the heart of C57BL/6 mice. Nanotoxicology 9:1013–1022. DOI: 10.3109/17435390.2014.996192. [PubMed: 25993494]

Ingber SZ, Pohl HR. 2016. Windows of sensitivity to toxic chemicals in the motor effects development. Regul Toxicol Pharmacol 74:93–104. DOI: 10.1016/j.yrtph.2015.11.018. [PubMed: 26686904]

Jalili P, Huet S, Lanceleur R, Jarry G, Le Hegarat L, Nesslany F, Hogeveen K, Fessard V. 2020. Genotoxicity of Aluminum and Aluminum Oxide Nanomaterials in Rats Following Oral Exposure. Nanomaterials (Basel) 10. DOI: 10.3390/nano10020305.

Kim YS, Kim JS, Cho HS, Rha DS, Kim JM, Park JD, Choi BS, Lim R, Chang HK, Chung YH, Kwon IH, Jeong J, Han BS, Yu IJ. 2008. Twenty-eight-day oral toxicity, genotoxicity, and gender-related tissue distribution of silver nanoparticles in Sprague-Dawley rats. Inhalation toxicology 20:575–583. DOI: 10.1080/08958370701874663. [PubMed: 18444010]

Krause BC, Kriegel FL, Rosenkranz D, Dreiack N, Tentschert J, Jungnickel H, Jalili P, Fessard V, Laux P, Luch A. 2020. Aluminum and aluminum oxide nanomaterials uptake after oral exposure - a

comparative study. Scientific reports 10:2698. DOI: 10.1038/s41598-020-59710-z. [PubMed: 32060369]

Kumari M, Kumari SI, Grover P. 2014. Genotoxicity analysis of cerium oxide micro and nanoparticles in Wistar rats after 28 days of repeated oral administration. Mutagenesis 29:467–479. DOI: 10.1093/mutage/geu038. [PubMed: 25209125]

Lecce JG, Broughton CW. 1973. Cessation of uptake of macromolecules by neonatal guinea pig, hamster and rabbit intestinal epithelium (closure) and transport into blood. The Journal of nutrition 103:744–750. [PubMed: 4122813]

Lee JH, Kim YS, Song KS, Ryu HR, Sung JH, Park JD, Park HM, Song NW, Shin BS, Marshak D, Ahn K, Lee JE, Yu IJ. 2013. Biopersistence of silver nanoparticles in tissues from Sprague-Dawley rats. Part Fibre Toxicol 10:36. DOI: 10.1186/1743-8977-10-36. [PubMed: 24059869]

Lenz KM, Nugent BM, McCarthy MM. 2012. Sexual differentiation of the rodent brain: dogma and beyond. Front Neurosci 6:26. DOI: 10.3389/fnins.2012.00026. [PubMed: 22363256]

Loeschner K, Hadrup N, Qvortrup K, Larsen A, Gao X, Vogel U, Mortensen A, Lam HR, Larsen EH. 2011. Distribution of silver in rats following 28 days of repeated oral exposure to silver nanoparticles or silver acetate. Part. Fibre Tox 8:18–31.

Mayer EA. 2011. Gut feelings: the emerging biology of gut-brain communication. Nature reviews. Neuroscience 12:453–466. DOI: 10.1038/nrn3071. [PubMed: 21750565]

Mayer EA, Tillisch K. 2011. The brain-gut axis in abdominal pain syndromes. Annual review of medicine 62:381–396. DOI: 10.1146/annurev-med-012309-103958.

Michael B, Yano B, Sellers RS, Perry R, Morton D, Roome N, Johnson JK, Schafer K, Pitsch S. 2007. Evaluation of organ weights for rodent and non-rodent toxicity studies: a review of regulatory guidelines and a survey of current practices. Toxicol Pathol 35:742–750. DOI: 10.1080/01926230701595292. [PubMed: 17849357]

Miller AH, Haroon E, Raison CL, Felger JC. 2013. Cytokine targets in the brain: impact on neurotransmitters and neurocircuits. Depress Anxiety 30:297–306. DOI: 10.1002/da.22084. [PubMed: 23468190]

Nakai JS, Elwin J, Chu I, Marro L. 2005. Effect of anaesthetics[sol]terminal procedures on neurotransmitters from non-dosed and aroclor 1254-dosed rats. J Appl Toxicol 25:224–233. DOI: 10.1002/jat.1058. [PubMed: 15856530]

Consumer Products Inventory: An inventory of nanotechnology-based consumer products introduced on the market. Woodrow Wilson International Center for Scholars. [11 18th, 2019 2019]

Nel A, Xia T, Madler L, Li N. 2006. Toxic potential of materials at the nanolevel. Science (New York, N.Y.) 311:622–627. DOI: 10.1126/science.1114397.

Nel A, Xia T, Meng H, Wang X, Lin S, Ji Z, Zhang H. 2013. Nanomaterial toxicity testing in the 21st century: use of a predictive toxicological approach and high-throughput screening. Accounts of chemical research 46:607–621. DOI: 10.1021/ar300022h. [PubMed: 22676423]

NRC. 2011. GUIDE FOR THE CARE AND USE OF LABORATORY ANIMALS. Institute for Laboratory Animal Research: The National Academy Press, Washington D.C.;

Pacha J 2000. Development of Intestinal Transport Function in Mammals. PHYSIOLOGICAL REVIEWS 80:1643–1667.

Pandey S, Singh A, Chaudhari N, Nampoothiri LP, Kumar GN. 2015. Protection against 1,2-di-methylhydrazine-induced systemic oxidative stress and altered brain neurotransmitter status by probiotic Escherichia coli CFR 16 secreting pyrroloquinoline quinone. Curr Microbiol 70:690–697. DOI: 10.1007/s00284-014-0763-9. [PubMed: 25586077]

Park EJ, Lee GH, Yoon C, Jeong U, Kim Y, Cho MH, Kim DW. 2016. Biodistribution and toxicity of spherical aluminum oxide nanoparticles. Journal of applied toxicology : JAT 36:424–433. DOI: 10.1002/jat.3233. [PubMed: 26437923]

Park EJ, Sim J, Kim Y, Han BS, Yoon C, Lee S, Cho MH, Lee BS, Kim JH. 2015. A 13-week repeated-dose oral toxicity and bioaccumulation of aluminum oxide nanoparticles in mice. Archives of toxicology 89:371–379. DOI: 10.1007/s00204-014-1256-0. [PubMed: 24798085]

Piao Y, Liu Y, Xie X. 2013. Change trends of organ weight background data in sprague dawley rats at different ages. J Toxicol Pathol 26:29–34. DOI: 10.1293/tox.26.29. [PubMed: 23723565]

Picut CA, Coleman GD. 2016. Chapter 5 - Gastrointestinal Tract. In Atlas of Histology of the Juvenile Rat, Parker GA, Picut CA (eds). Academic Press: Boston; 127–171

Rollerova E, Jurcovicova J, Mlynarcikova A, Sadlonova I, Bilanicova D, Wsolova L, Kiss A, Kovriznych J, Kronek J, Ciampor F, Vavra I, Scsukova S. 2015. Delayed adverse effects of neonatal exposure to polymeric nanoparticle poly(ethylene glycol)-block-polylactide methyl ether on hypothalamic-pituitary-ovarian axis development and function in Wistar rats. Reproductive toxicology (Elmsford, N.Y.) 57:165–175. DOI: 10.1016/j.reprotox.2015.07.072.

Saunders NR, Dreifuss JJ, Dziegielewska KM, Johansson PA, Habgood MD, Mollgard K, Bauer HC. 2014. The rights and wrongs of blood-brain barrier permeability studies: a walk through 100 years of history. Front Neurosci 8:404. DOI: 10.3389/fnins.2014.00404. [PubMed: 25565938]

Saunders NR, Habgood MD, Dziegielewska KM. 1999. Barrier mechanisms in the brain, II. Immature brain. Clin Exp Pharmacol Physiol 26:85–91. [PubMed: 10065326]

Saunders NR, Liddelow SA, Dziegielewska KM. 2012. Barrier mechanisms in the developing brain. Front Pharmacol 3:46. DOI: 10.3389/fphar.2012.00046. [PubMed: 22479246]

Semmler-Behnke M, Kreyling WG, Schulz H, Takenaka S, Butler JP, Henry FS, Tsuda A. 2012. Nanoparticle delivery in infant lungs. Proceedings of the National Academy of Sciences of the United States of America 109:5092–5097. DOI: 10.1073/pnas.1119339109. [PubMed: 22411799]

Semple BD, Blomgren K, Gimlin K, Ferriero DM, Noble-Haeusslein LJ. 2013. Brain development in rodents and humans: Identifying benchmarks of maturation and vulnerability to injury across species. Prog Neurobiol 106–107:1–16. DOI: 10.1016/j.pneurobio.2013.04.001.

Shrivastava R, Raza S, Yadav A, Kushwaha P, Flora SJ. 2014. Effects of sub-acute exposure to TiO2, ZnO and Al2O3 nanoparticles on oxidative stress and histological changes in mouse liver and brain. Drug Chem Toxicol 37:336–347. DOI: 10.3109/01480545.2013.866134. [PubMed: 24344737]

Song C, Manku MS, Horrobin DF. 2008. Long-Chain Polyunsaturated Fatty Acids Modulate Interleukin-1b–Induced Changes in Behavior, Monoaminergic Neurotransmitters, and Brain Inflammation in Rats. J. Nutr 138:954–963. [PubMed: 18424607]

SoRelle ED, Liba O, Campbell JL, Dalal R, Zavaleta CL, de la Zerda A. 2016. A hyperspectral method to assay the microphysiological fates of nanomaterials in histological samples. Elife 5. DOI: 10.7554/eLife.16352.

Teichberg S, Wapnir RA, Moyse J, Lifshitz F. 1992. Development of the neonatal rat small intestinal barrier to nonspecific macromolecular absorption. II. Role of dietary corticosterone. Pediatric research 32:50–57. DOI: 10.1203/00006450-199207000-00010. [PubMed: 1635845]

Tietz T, Lenzner A, Kolbaum AE, Zellmer S, Riebeling C, Gurtler R, Jung C, Kappenstein O, Tentschert J, Giulbudagian M, Merkel S, Pirow R, Lindtner O, Tralau T, Schafer B, Laux P, Greiner M, Lampen A, Luch A, Wittkowski R, Hensel A. 2019. Aggregated aluminium exposure: risk assessment for the general population. Archives of toxicology 93:3503–3521. DOI: 10.1007/s00204-019-02599-z. [PubMed: 31659427]

Westrom BR, Svendsen J, Karlsson BW. 1982. Protease inhibitor levels in porcine mammary secretions. Biology of the neonate 42:185–194. [PubMed: 6182928]

Westrom BR, Tagesson C, Leandersson P, Folkesson HG, Svendsen J. 1989. Decrease in intestinal permeability to polyethylene glycol 1000 during development in the pig. Journal of developmental physiology 11:83–87. [PubMed: 2476476]

Willhite CC, Karyakina NA, Yokel RA, Yenugadhati N, Wisniewski TM, Arnold IM, Momoli F, Krewski D. 2014. Systematic review of potential health risks posed by pharmaceutical, occupational and consumer exposures to metallic and nanoscale aluminum, aluminum oxides, aluminum hydroxide and its soluble salts. Crit Rev Toxicol 44 Suppl 4:1–80. DOI: 10.3109/10408444.2014.934439.

Wisser J, Horster M. 1978. In vitro perfused, non-isolated small intestine: ontogeny of transmural hydraulic permeability. Pflugers Archiv : European journal of physiology 373:205–208. [PubMed: 565047]

Yin N, Zhang Y, Yun Z, Liu Q, Qu G, Zhou Q, Hu L, Jiang G. 2015. Silver nanoparticle exposure induces rat motor dysfunction through decrease in expression of calcium channel protein in

cerebellum. Toxicology letters 237:112–120. DOI: 10.1016/j.toxlet.2015.06.007. [PubMed: 26068065]

Younoszai MK, Sapario RS, Laughlin M. 1978. Maturation of jejunum and ileum in rats. Water and electrolyte transport during in vivo perfusion of hypertonic solutions. The Journal of clinical investigation 62:271–280. DOI: 10.1172/jci109126. [PubMed: 670394]

Zhang XF, Gurunathan S, Kim JH. 2015. Effects of silver nanoparticles on neonatal testis development in mice. International journal of nanomedicine 10:6243–6256. DOI: 10.2147/ijn.s90733. [PubMed: 26491295]

	Dynamic Light Scattering (DLS)		Nanoparticle Tracker (NTA)	
Time (h)	Hydrodynamic Diameter (nm)	Polydispersity index (PdI)	Mean diameter (nm)	Mode (nm)
0	148 ± 1.3	0.124	191 ± 96	111
4	151 ± 2.1	0.131	213 ± 72	106
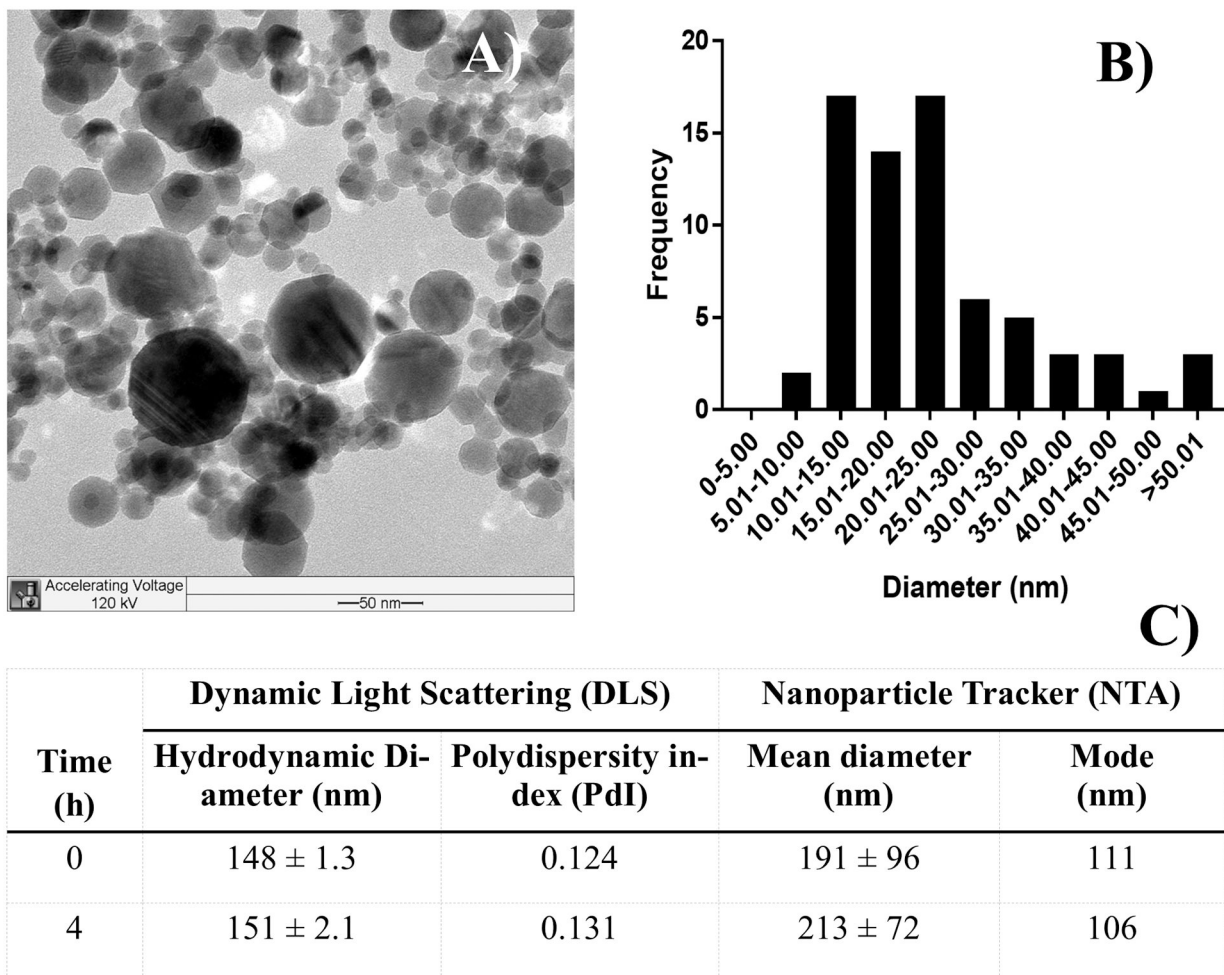
Figure 1.
A) TEM image of Al_2O_3 NP and B) size distribution. C) Characterization of the 2 mg/mL dosing solutions was done by DLS and NTA at 0 and 4 hours after preparation.
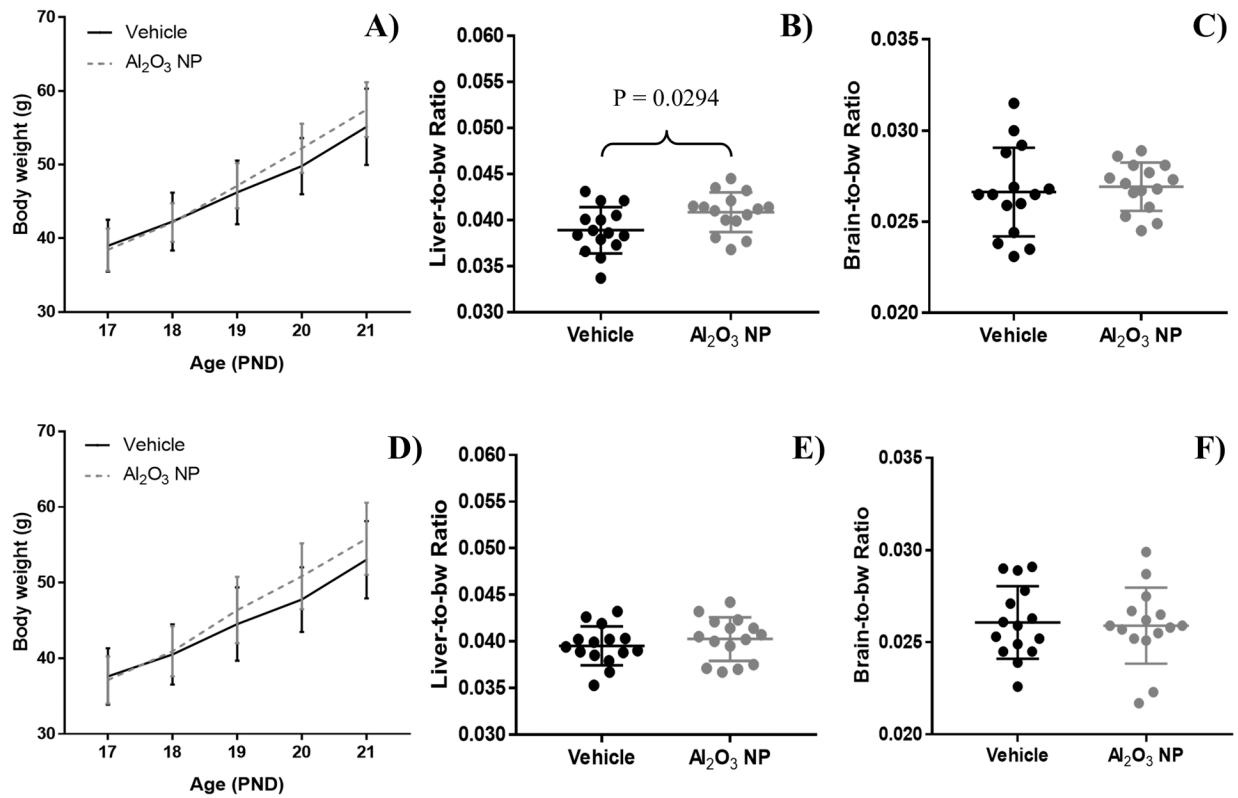
Figure 2.
Body weight (bw) for A) male and D) female pups dosed with Al_2O_3 NP (dotted line) and vehicle control (solid line) between PND 17–20. Pups were sacrificed on PDN 21, and the liver-to-bw ratio for B) male and E) female and brain-to-bw ratio for C) male and F) female pups were calculated. In male pups Al_2O_3 NP administration caused a significant increase in liver-to-bw ratio. The graphs show mean ± standard deviation.
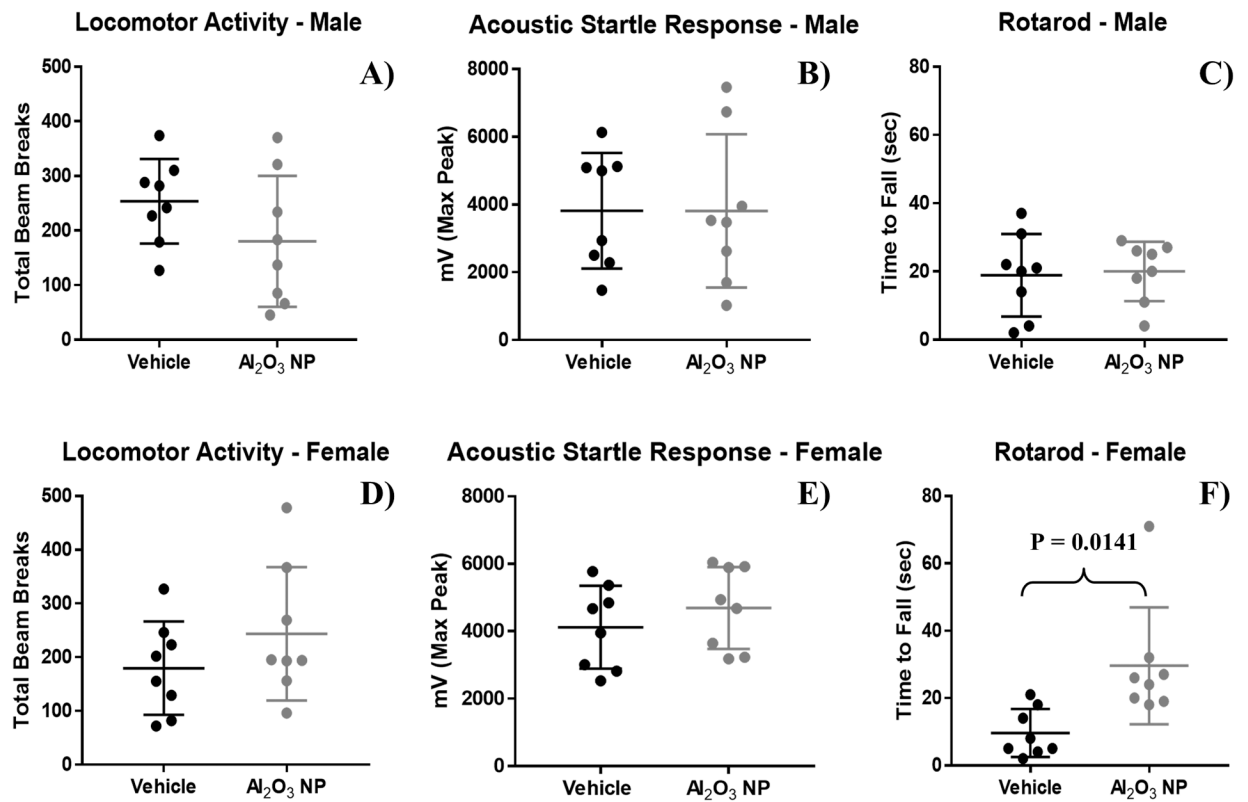
Figure 3.
Basic neurobehavioral assessment of A-C) male and D-F) female pups administered Al_2O_3 NP were performed by measuring A+D) locomotor activity, B+E) acoustic startle response, and C+F) rotarod, showing mean ± standard deviation.
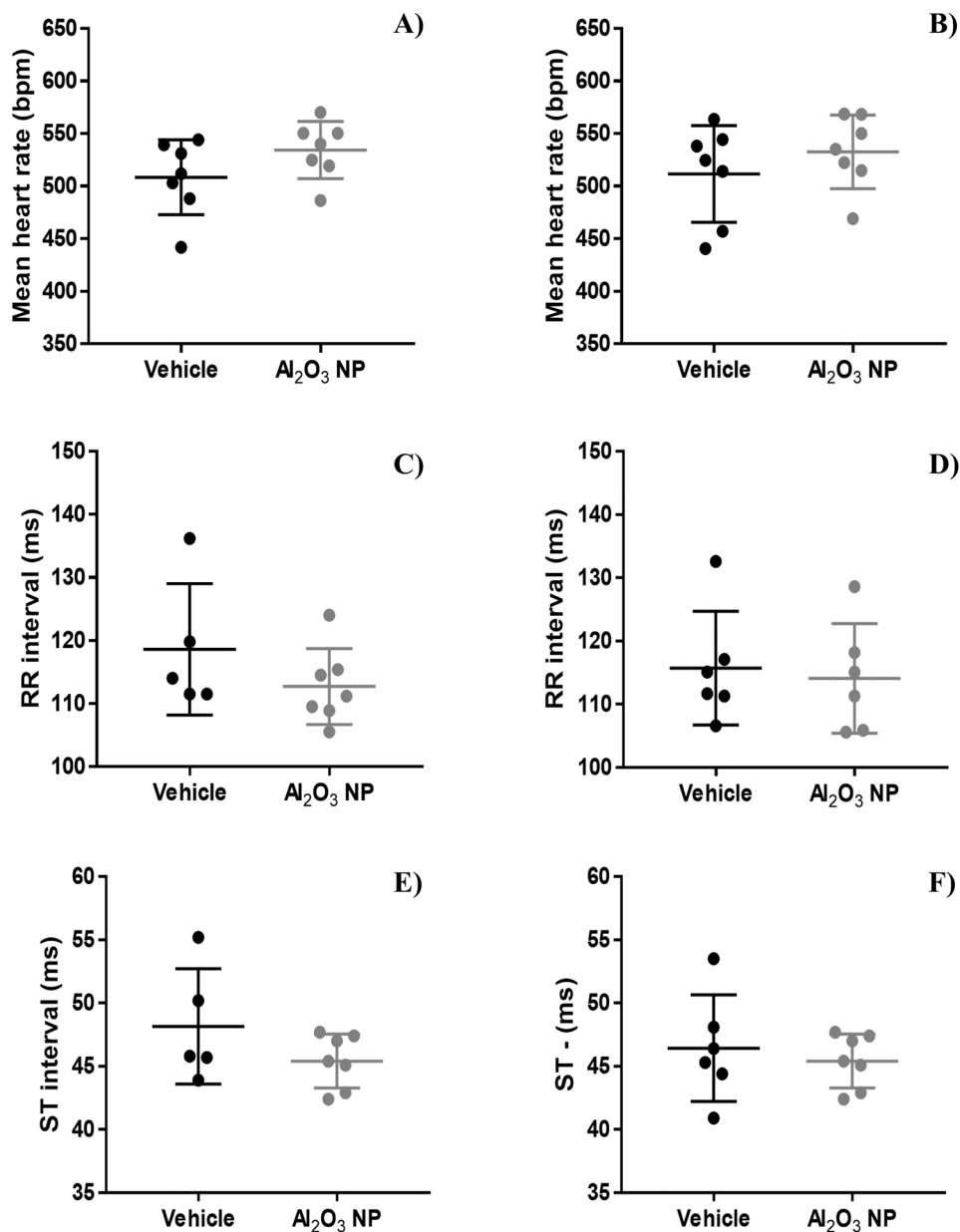
Figure 4.

The electrocardiograms for unrestrained and awake male and female pups were performed non-invasively by ECGenie over a period of 10 min. No significant change was observed for A-B) heart rate (beat per minute [bpm]), C-D) RR interval (milliseconds [ms]), or E-F) ST interval (milliseconds [ms]) as a result of Al_2O_3 NP oral exposure. The graphs show mean ± standard deviation.
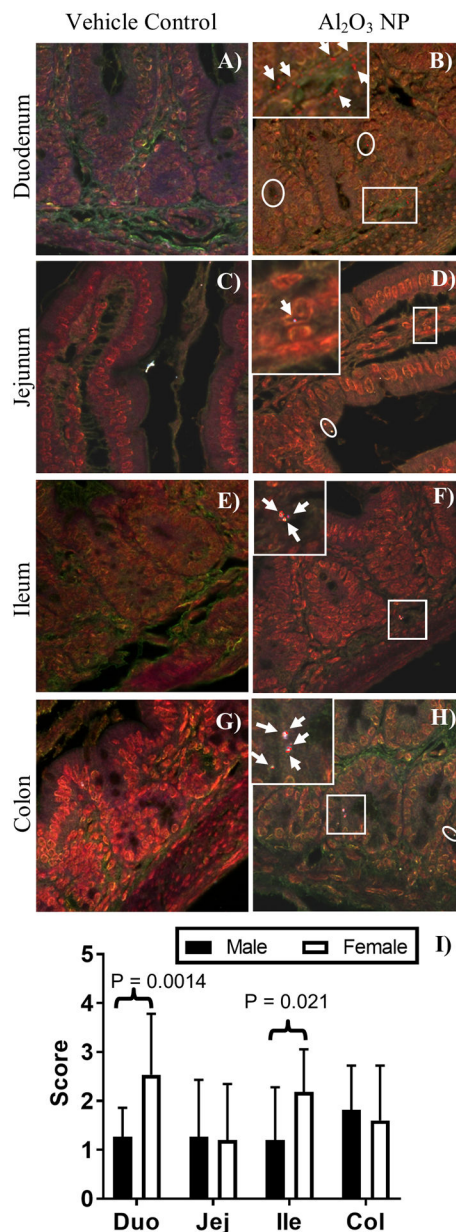
Figure 5.
Hyperspectral images of H&E stained vehicle control and Al_2O_3 NP dosed A-B) duodenum, C-D) jejunum, E-F) ileum, and G-H) colon. Mapped areas are highlighted in the HSI images and indicated by white circles. A magnification outlined with a white square is inserted for each of the Al_2O_3 NP tissues to show the cellular location of NPs and the mapped areas are shown with white arrows. A, C, E, F) are male tissues and B, D, G, H) are female tissues, no visible differences were observed between male and female tissues. The presence of NPs was scored in the tissue: 0 = no NP signals detected; 1 = 1 – 10 NP signals detected; 2 = 11 – 25 NP signals detected; 3 = 26 – 50 NP signals detected; 4 = 51 – 100 NP signals detected; 5 = >100 NP signals detected. I) The score for Al_2O_3 NP was higher in female duodenum

and ileum than for male pups. The score for males is shown in black bars and the score for females in white bars, showing mean ± standard deviation
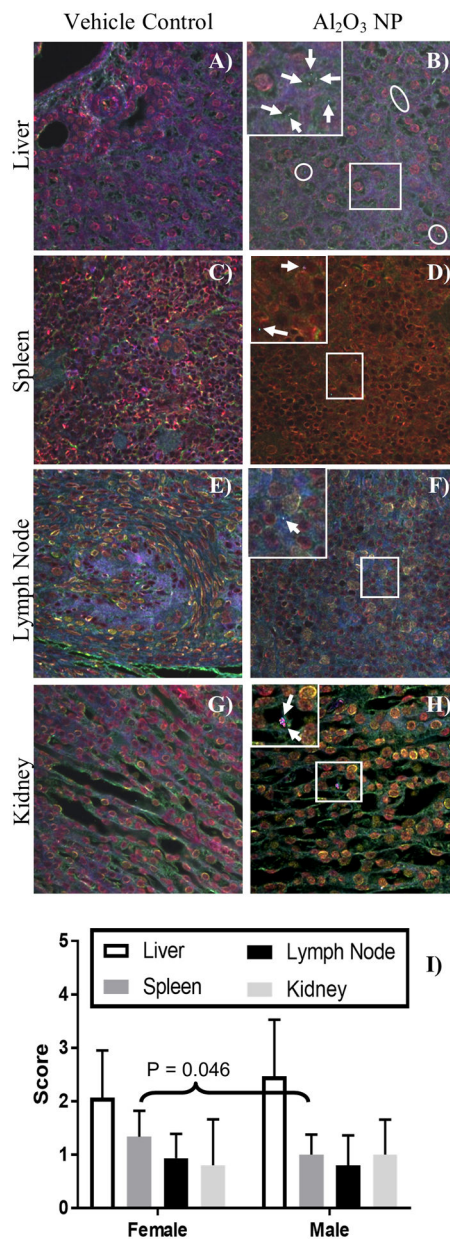
Figure 6.
Hyperspectral images of H&E stained vehicle control and Al_2O_3 NP dosed A-B) liver, C-D) spleen, E-F) lymph node, and G-H) kidney. Mapped areas are highlighted in the HSI images and indicated by circles. A magnification outlined with a white square is inserted for each of the Al_2O_3 NP tissues to show the cellular location of NPs and the mapped areas are shown with white arrows. A, C, D, E, G, H) are male tissues and B, F) are female tissues, no visible differences were observed between male and female tissues. The presence of Al_2O_3 NP was scored in the tissues: 0 = no NP signals detected; 1 = 1 – 10 NP signals detected; 2 = 11 – 25 NP signals detected; 3 = 26 – 50 NP signals detected; 4 = 51 – 100 NP signals detected; 5 = >100 NP signals detected. The score for Al_2O_3 NP was highest in the liver compare to spleen, lymph nodes, and kidney, showing mean ± standard deviation
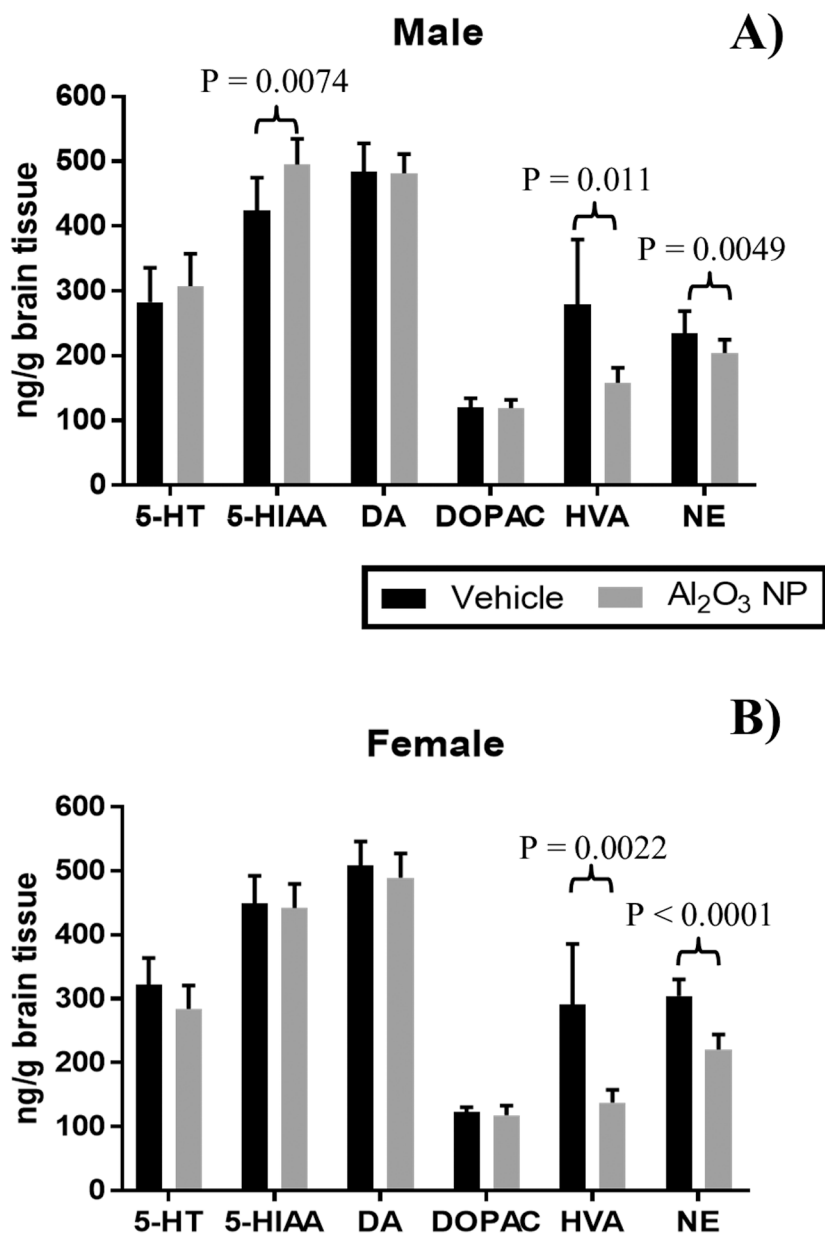
Figure 7.
Concentration of six neurotransmitters: Serotonin or 5-hydroxytryptamine (5-HT), 5-Hydroxyindoleacetic acid (5-HIAA), dopamine (DA), 3,4-Dihydroxyphenylacetic acid (DOPAC), homovallinic acid (HVA), and norepinephrine (NE) were determined in the right brain half in A) male and B) female juvenile rats, showing mean ± standard deviation. The concentrations of HVA and NE was significantly decreased in the brain for both male and female pups, while 5-HIAA was increased only in male pups.